Thermal Performance Characterization of Embedded Pulsating Heat Pipe Radiators by Infrared Thermography

Vadiraj A. Hemadri[1], Sameer Khandekar[2]

1: Dept. of Mechanical Engineering, IIT Kanpur, India, vadiraj@iitk.ac.in
2: Dept. of Mechanical Engineering, IIT Kanpur, India, samkhan@iitk.ac.in

Abstract This experimental study investigates the thermal performance of Closed Loop Pulsating Heat pipe (CLPHP) embedded radiator plates subjected to conjugate heat transfer conditions, i.e. natural convection and radiation. The performance of the plate is studied for different geometrical orientations of the CLPHP. High speed, high resolution infrared camera is used to obtain real-time thermal images and spatial temperature profiles of the radiator plate. The study reveals that the relative advantage of embedded radiator plates is appreciably higher if the thermal conductivity of the base plate is low. It is possible to appreciably enhance the performance of low thermal conductivity material by embedding PHP structure.

Keywords: Pulsating Heat Pipes, Space Radiators, Conjugate Heat Transfer

1. Introduction

Radiators are an essential part of any space application. Many space radiator designs are available at present (Gilmore, 2002). Although they meet the present requirements of the industry, future applications envisage higher heat flux levels. In this background, the feasibility of using pulsating heat pipes in an aluminum radiator plate as integrated heat spreaders has been studied by Khandekar and Gupta (2007). The literature suggests that such embedded structures are beneficial under certain conditions. It also predicts based on computational simulation that the decrease in internal thermal resistance of the plate is significant with a substrate of lower thermal conductivity. This work investigates the performance of embedded radiator plates with two different substrates using infrared thermography. To understand the effectiveness of the embedded PHP system, let us first approach the problem with a 1-D point of view. The heat transfer through the plate along with the various resistances as given by Kaviany (2001):

$$(T_1 - T_2) / q''_{cond} = R_{th}|_{conduction} = \Delta x / k_{plate} \quad (1a)$$

$$(T_2 - T_\infty) / q''_{conv} = R_{th}|_{convection} = 1/h \quad (1b)$$

$$(T_2 - T_\infty) / q''_{rad} = R_{th}|_{radiation} = (\sigma_r . T_m)^{-1} \quad (1c)$$

Where,

$$T_m = \left[(T_2^2 + T_\infty^2)(T_2 + T_\infty) \right]$$

The Effective Biot Number ($\overline{Bi}$) compares the internal thermal resistance of the plate to the total external resistance.

$$\overline{Bi} = \frac{\text{internal conductive resistance}}{\text{natural convective resistance + radiation}}$$

$$= \frac{(\Delta x / k_{plate})}{(1/h) + (\sigma_r . T_m)^{-1}} \quad (2)$$

If the effective Biot number is small ($\overline{Bi}$ <0.1) the conductive resistance is negligible and the heat transfer is primarily dependent on the external transfer coefficient. This is usually the case with materials of high thermal conductivity subjected to natural convection. To increase the heat transfer, each of the resistances mentioned above (in eq. 1a, 1b and 1c) should be reduced.

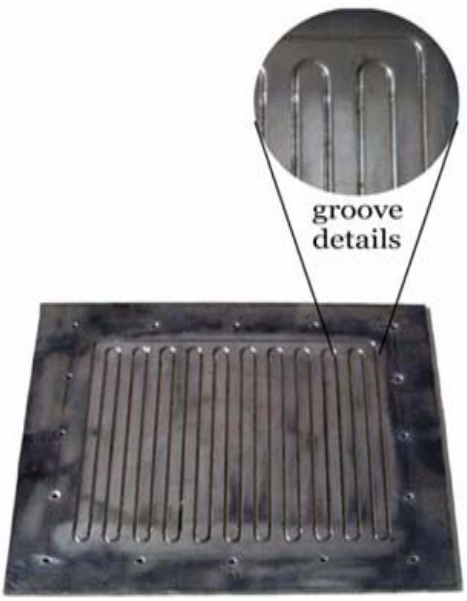

Fig. 1. Radiator plate with groove details

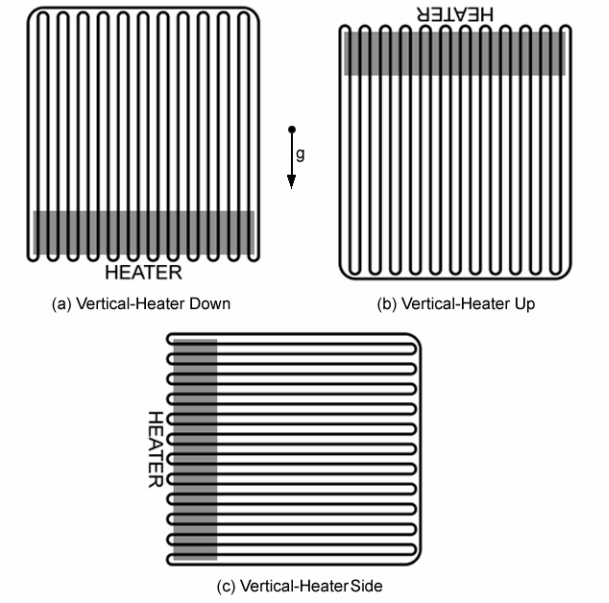

Fig. 2. Different orientations of the plate

In the present work, effort is made to reduce the conductive resistance of the plate by the application of embedded pulsating heat pipes. The experiments were performed on mild steel and aluminum base plates and after obtaining satisfactory results with the mild steel plate, it was further tested at different orientations (Fig.2). All the experiments were performed for vertical position of the plate. The images obtained by infrared camera depict the degree of isothermalization of the base plate.

2. Experimental details

The experiments were performed on aluminum and mild steel plates with dimensions 350 x 350 x 5 mm^3, as shown in Fig.1. Semi circular grooves were milled on the plates into which capillary tube made of copper (ID/OD: 2.0/3.0mm, length 255 mm and inter tube pitch 12.mm, 11 turns on each end, internal volume 17.5 cc) was embedded with the application of a heat sink compound. The plate surface was coated black to obtain a high emissivity ($\varepsilon \approx 0.97$). Heat supply was given by a surface mountable flat mica heater (200 x 50 x 1 mm^3) mounted at the bottom of the base plate. For AC power supply, a continuously variable voltage auto-transformer coupled with a high precision digital multimeter was used.

Two precisely calibrated K-type thermocouples were used to validate the temperature readings obtained by the infrared camera. Data acquisition for the thermocouples was done by a 24-bit PC interface. The embedded CLPHP plate was mounted on a tiltable frame. A high speed, high resolution Forward Looking Infrared (FLIR) camera with a wavelength range of 3-5 μm was used to obtain real-time temperature profiles of the plate. The whole setup was enclosed in a 'black' enclosure to minimize the light reflected from the background. The experiment was performed with both water and ethanol as working fluids and the filling ratio (FR) was maintained at 60% throughout. Dry tests were carried out on the radiator plates, without any working fluid in the PHP, after evacuating the capillary tube. The heat input was varied from 50W to 150W. The spatial temperature distribution of the radiator plates was obtained by the infrared camera at quasi-steady state.

3. Results and Discussion

Fig.3 shows the temperature profiles of the aluminum plate at 120W for vertical heater down position, for dry test and with ethanol as working fluid respectively. The aluminum plate has an isothermal distribution even without a working fluid. A slightly better temperature

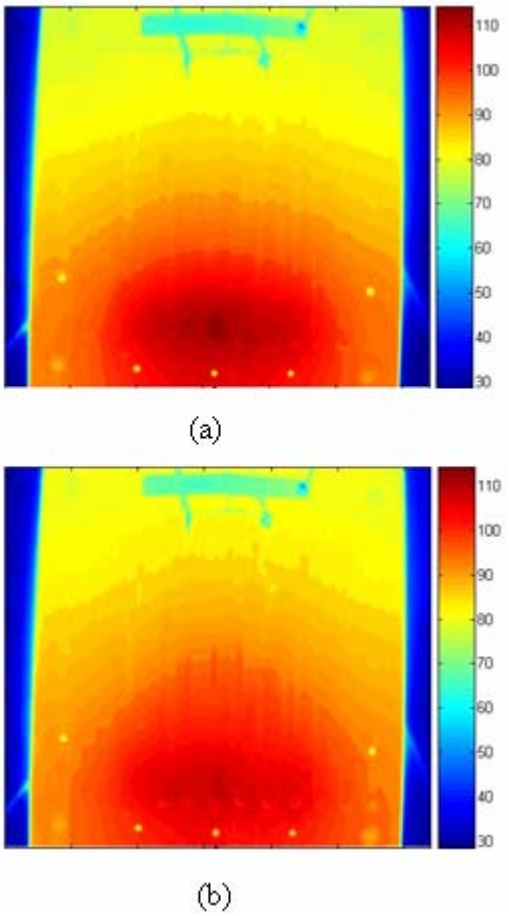

Fig. 3. Temperature profile of the aluminum base plate at 120W. (a) Dry test (b) with ethanol

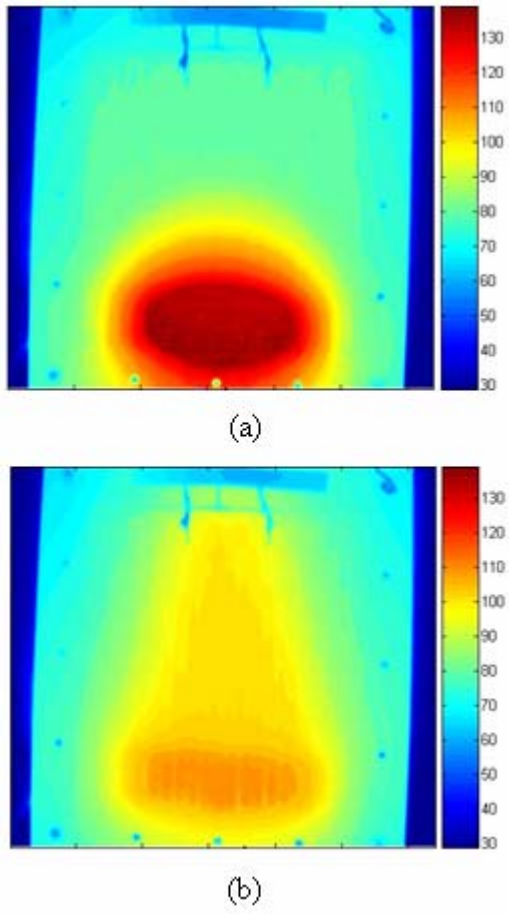

Fig. 4. Temperature profile of the mild steel base plate at 120W. (a) Dry test (b) with ethanol

distribution is obtained by the PHP action and its contribution is not very significant. It can be deduced from the observations that:

(1) The thermal conductivity of the aluminum base plate itself is very high, so the additional contribution due to the PHP action is not creating appreciable change.

(2) The radiator plate is quite thick (5.0 mm) thus reducing the thermal resistance of the plate leading to heat conduction in the spanwise direction.

(3) The advantage achieved by using CLPHP in a radiator plate asymptotically levels off as the thermal conductivity of the base plate increases. This is because the heat transfer is governed/limited by the external resistance i.e. convection, radiation or conjugate (Eq. 1 and 2). Therefore it is not advisable to invest in a technology that increases the thermal conductivity of the base plate beyond a particular limit.

Although the thermal performance of the CLPHP can never be as good as conventional heat pipes, they are much simpler and cheaper to fabricate (Khandekar, 2004). Also, PHPs are not affected by conventional heat pipe limitations (e.g. capillary limit). In this regard, the temperature profiles of the mild steel plate (Fig.4) which has comparatively lower thermal conductivity clearly depict the contribution of the embedded PHPs in the isothermalization of the radiator plate. As the result of PHP action there is significant reduction in the maximum temperature of the radiator plate (30° C).

3.1 Comparison of maximum plate temperature (T_{max})

A comparison of maximum temperature of the radiator plates provides a clear indication of the advantage achieved by the PHP action.

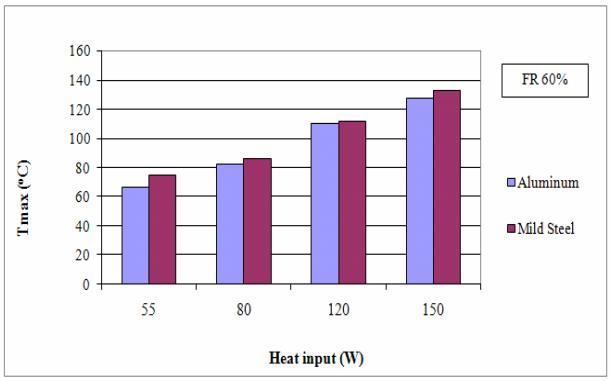

Fig. 5. Comparison of T_{max} for aluminum and mild steel plates with ethanol

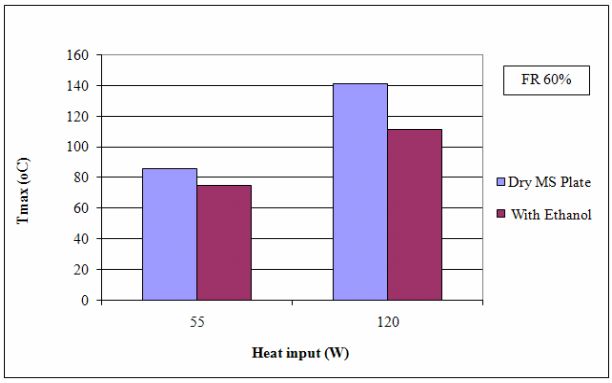

Fig. 6. Comparison of T_{max} for mild steel plate for dry test and with ethanol

Fig.5 shows the maximum temperature of aluminum and mild steel plates at different heat inputs. The values of T_{max} for both plates are comparable despite lower thermal conductivity of the mild steel plate. It is appreciably higher (30° C higher) in dry test (Fig. 6). In fact, at 120W, T_{max} is the same for both the plates with ethanol as working fluid. This implies that, for a given heat input, the mild steel plate behaves identically to an aluminum plate considering T_{max} (Fig. 3, 4). Therefore, in cases where T_{max} defines the design considerations, a suitable material which is mechanically superior to aluminum but thermally inferior could very well do the job with embedded PHP systems.

3.2 Variation of thermal resistance (R_{th})

Fig. 7 shows the variation of the thermal resistance of the embedded radiator plate with increase in heat input for vertical bottom heating orientation of the plate. The results indicate that R_{th} of such structures decreases with increase in heat flux, which is inline with

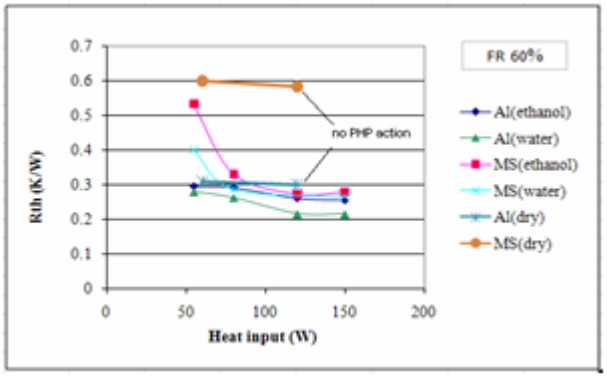

Fig. 7. Variation of R_{th} with heat input (vertical bottom heating orientation)

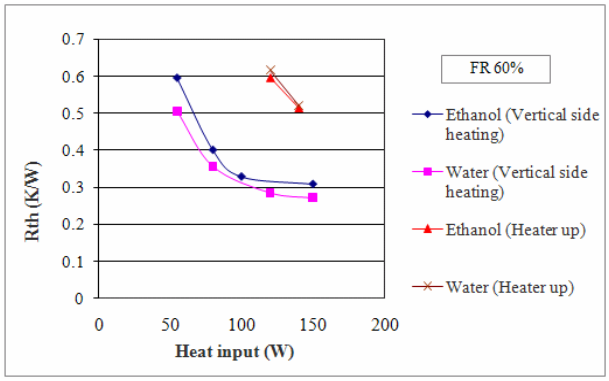

Fig. 8. Variation of R_{th} with heat input (vertical heater up and vertical side heating orientations)

earlier observations [e.g. Hosoda, Nishio and Shirakashi, 1999, Khandekar, Dollinger and Groll, 2003, Tong, Wong, and Ooi, 2001). This is due to the fact that the thermal power input is the driving force for the self sustained oscillations of the CLPHP. Also, the results are slightly better with water as working fluid. At 55W, the pulsations were minimal and R_{th} is very close to the dry tests. At higher heat inputs, R_{th} of the mild steel plate is reduced by almost 50% which reiterates that the CLPHP indeed plays a significant role in heat transfer for low thermal conductivity materials.

The performance of the mild steel plate was then further tested for vertical heater up and vertical side heating orientations. Fig. 8 shows the results of these tests. The performance of the plate in vertical side heating orientation was satisfactory and the variation of thermal resistance follows a similar trend as that of vertical bottom heating. However, for vertical heater up orientation the pulsating action was not continuous and hence the thermal resistance was comparatively higher.

3.3 Effect of orientation

Since the embedded structure is tested for its potential space applications where its orientation is arbitrary, experiments were also performed for vertical heater up and vertical side heating orientations of the plate.

At lower heat inputs, for vertical-heater up position, gravity adversely affected the performance and no pulsations were observed. With higher heat inputs the thermal driving forces dominated the gravity. The performance improved considerably and pulsations showed up intermittently at higher heat inputs thus reducing $R_{th..}$ Fig. 9 shows the snapshots of the radiator plate with and without PHP action in vertical-heater up position.

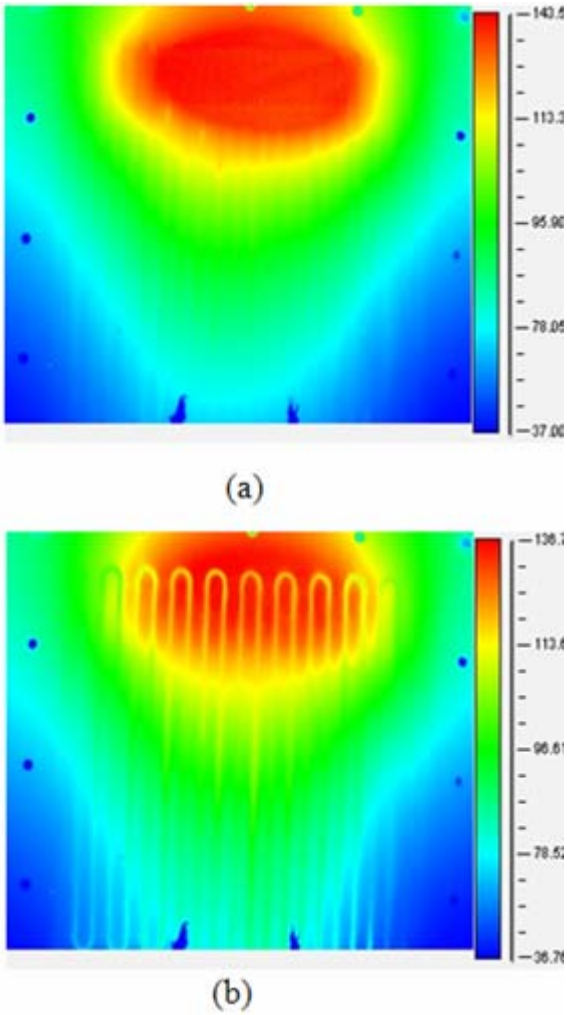

Fig. 9. Thermal profiles of the mild steel plate in vertical heater up orientation at 140W with water (a) Without PHP action (b) With PHP action.

The performance of the plate in vertical side heating orientation was satisfactory, with T_{max} comparable to that of vertical bottom heating orientations (Fig. 6 and Fig. 10). The variation of T_{max} was recorded at different orientations, at quasi steady state (Fig. 11) The magnitude of T_{max} as well as its amplitude of variation is very high in vertical heater up orientation as compared to the other two orientations as a result of intermittent operation.

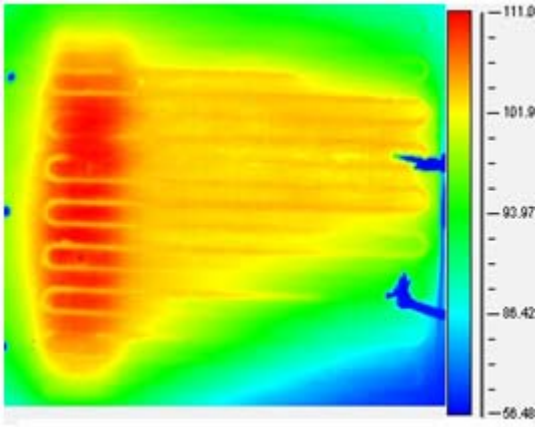

Fig. 10. Thermal profile of the mild steel plate in vertical side heating orientation at 120W with ethanol.

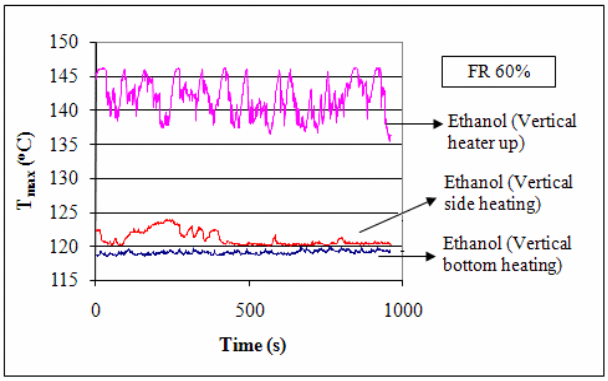

Fig. 11. Variation of T_{max} for mild steel plate at quasi-steady state for different orientations.

4. Conclusions

Infrared thermography was successfully employed to study the performance of CLPHP embedded radiator plates subjected to conjugate boundary condition for two different working fluids .i.e. ethanol and water. The effect of orientation of the plate on its thermal performance was also studied. The following are the major conclusions:

(1) The use of CLPHP resulted in a considerable decrease in the thermal resistance of the mild steel plate as predicted by the simulation results obtained by Khandekar S. et al. [5] The advantage obtained by embedding CLPHP is significant if the thermal conductivity of the base plate is low. As the thermal conductivity of the base plate increases the Biot Number decreases and the heat transfer is mainly governed by the external heat transfer co-efficient (e.g. aluminum). In such cases the base plate itself does a god job and further addition of CLPHP only marginally increases the performance.
(2) The T_{max}, in the case of aluminum and mild steel plates, were comparable at higher heat fluxes. Therefore, if T_{max} governs the design considerations, the behavior of both the plates is identical. In such cases, a composite material having a weight/strength advantage over aluminum but thermally inferior could be considered as an option. This is a very attractive option for space applications.
(3) The inclination operating angle of the PHP tubes changes the internal flow patterns and changes the performance levels. Increasing heat flux makes these performances comparable.

Nomenclature

Bi Biot Number = hL_c/ K_s
D diameter (m)
FR Volumetric filling ratio(V_{liq}/V_{total})
g acceleration due to gravity (m/s^2)
h heat transfer coefficient (W/m^2k)
k thermal conductivity (W/mk)
L length (m)
q" heat flux (W/m^2)
R_{th} thermal resistance (Km^2/W)
T temperature ($^\circ$C or K)

Greek symbols

ε surface emissivity
σ_r Stefan-Boltzman Constant = 5.67e-8W/m^2K^4
ρ density(kg/m^3)

Subscripts

∞ ambient
c characteristic
liq liquid
s solid

References

Gilmore G. David, 2002. Spacecraft Control Handbook, Vol.-1: Fundamental Technologies, The Aerospace Corporation (AIAA Publication), ISBN: 1-884989-11-X (v.1), 2nd Edition.

Holley B. and Faghri A., 2005. Analysis of Pulsating Heat Pipe with Capillary Wick and Varying Channel Diameter, Int. J. of Heat and Mass Transfer, Vol. 48 (13), pp. 2635-2651.

Hosoda M., Nishio S. and Shirakashi R., 1999. Study of Meandering Closed-Loop Heat-Transport Device, JSME Int. Journal, Series B, Vol. 42, No. 4, pp. 737-743.

Kaviany M., 2001. Principles of Heat Transfer, ISBN: 0471434639, Wiley- Interscience.

Khandekar S. and Gupta A., 2007. Embedded Pulsating Heat Pipe Radiators, 14th International Heat pipe Conference (14th IHPC), Florianopolis, Brazil.

Khandekar S., 2004. Thermo-hydrodynamics of Closed Loop Pulsating Heat Pipes, Ph.D. dissertation, Universitat Stuttgart, Germany.

Khandekar S., Dollinger N. and Groll M., 2003. Understanding Operational Regimes of Pulsating Heat Pipes: An Experimental Study, Applied Thermal Engg., Vol. 23/6, pp-707-719.

Tong B., Wong T., and Ooi K., 2001. Closed-Loop Pulsating Heat Pipe, Applied Thermal Engg., Vol. 21, No. 18, pp. 1845-1862.